JEE Journal of Ecological Engineering

*Journal of Ecological Engineering*, 2025, 26(7), 329–342
https://doi.org/10.12911/22998993/203522
ISSN 2299–8993, License CC-BY 4.0

Received: 2025.03.06
Accepted: 2025.04.30
Published: 2025.05.15

# Mechanical and tribological properties of bovine hoof powder reinforced polyurethane composites

Kumar Duraisamy[1*], Syed Amjad Ahmed[1], Kumaran Chinnasamy[1], Abdul Hakim Javid[1]

[1] Department of Mechanical Engineering, C. Abdul Hakeem College of Engineering and Technology, Melvisharam, 632509, India

* Corresponding author's e-mail: kumard.mech@cahcet.edu.in

## ABSTRACT

This paper intended to discuss the fabrication and evaluation of mechanical as well as tribological properties of biowaste-based composites. The biowaste employed in the present work is bovine hoof. In this work, bovine hoof powder (BHP)-reinforced polyurethane composites were fabricated using varying weight percentages (0%, 2.5%, 5%, 7.5%, 10% and 15%) of bovine hoof powder, polyol and isocyanate. The bovine hoof powder is processed by cleaning, milling, pulverizing, sieving, washing, defatting and treating with 0.1N NaOH solution. The composites were fabricated by mixing polyether polyol, bovine hoof powder and toluene diisocyanate (TDI) hardener and pouring into a die followed by curing at higher temperature. The mechanical and tribological properties of the composites were studied on the composites. It was observed that properties such as tensile strength, tensile modulus, coefficient of friction, density, porosity, oil absorption and water absorption of the composite specimens increase along with the bovine hoof powder loading. In contrast, properties such as wear rate, hardness and impact strength of the composites decrease with increase in BHP loading. With increase in loading of bovine hoof powder from pure polyurethane, it was observed that the stiffening-softening-stiffening behavior of composites occurred. It was observed that the optimum weight % of bovine hoof powder loading amounts to 7.5% by weight. The BHP composites indicated enhanced hydrophilicity. Furthermore, the FTIR analysis demonstrated significant degradation in the presence of UV radiation and an oxidation process at 1724cm$^{-1}$ and 1600 cm$^{-1}$. The photolytic and hydrolytic effects were also found to cause microcracks. Accordingly, it may be inferred that the properties of the proposed composites are appropriate to applications like foot wear and related fields. Since the raw material used for the fabrication of the proposed composite is derived from biowaste, the resulting composite is not only eco-friendly, but also aligns with the United Nations – Sustainable Development Goals (SDGs).

**Keywords:** composites, polyurethane, bovine-hoof powder, properties.

## INTRODUCTION

Fabrication of polymer composites using biowaste from animals, attracts attention due to its biodegradable nature and reduction in environmental pollution. These composites become alternative to synthetic fiber-reinforced polymer composites. Bovine hooves are found at the tip of toe of cattle, sheep, goat, etc. Hoof supports the weight and provides traction for the animals. Hooves dissipate the impact energy of the animal while interacting with the ground and protect the bone as well as tissue. Bovine hooves are tough and are made of fibrous hard alpha-keratin that is alpha-helical coiled coil in structure that is rich in sulfur content. Bovine hoof is one type of the slaughterhouse biowaste that is discarded causing land and water pollution. Employing such animal waste for the fabrication of polymer composites may facilitate both economic and social sustainable development (Issa et al., 2020). Therefore, towards utilization of these biowaste, many investigations were conducted to evaluate the usage in the form of composites.

### Bovine hoof powder as reinforcement

When investigating the tribological behavior of phenolic resin composites reinforced with bagasse and cow hoof dust, Olokode et al. (2012) found that the dust of the hooves adhered with bagasse and provided strength and resistance to heat at the friction interface. However, the strength and the resistance was quite low with one reinforment. The tribological behavior of horn powder-reinforced epoxy composites was optimized using GRA and ANOVA. From the investigation, it was observed that the optimum factors were 30% volume fraction, 425 μm sized particles, 0.1 N NaOH concentration (Kumar et al., 2016). Later, the evaluation of mechanical behavior of bio-waste horn powder reinforced epoxy composites by (Kumar et al., 2017) found that horn powder loading influences more than horn powder particle size and concentration of NaOH. Kumar and Rajendraboopathy (2014) analyzed the properties of composites fabricated using treated horn powder and polypropylene and found that the optimum weight percentage of horn powder particles in polypropylene matrix is 15%.

Huang et al. (2019) studied the structure and energy absorbing mechanism of hoof wall. It was observed that the hardness and stiffness of the hoof at the inter tubular area decrease with increase in hydration than at tubular areas. The compression test of the hoof at various loading rate and direction show that the strength and stiffness are lower at high speeds and in radial directions than at other directions. It was also observed that the hardness and modulus of the hoof decreases due to hydration. Using horn powder as reinforcement, Kumar et al. (2020) optimized the thermal and mechanical properties of horn powder and phenol formaldehyde reinforced composites. From the analsyis, it was documented that the optimal factors were 0.1 N NaOH concentration, 125 μm horn powder particle size and 10% horn powder volume content. Similarly, Baillie et al., (2000) investigated the fracture behavior and bending stiffness of bovine hoof at different orientations and levels of hydration. A decrease in stiffness when increasing the moisture content was observed along the direction of intermediate filaments and tubules.

Also, there are investigations that have documented that the change in the matrix and reinforcements resulted in the enhancement of the physical properties. For instance, employing glass and carbon fiber-reinforced polyol, Olszewski et al. (2021) observed that there were increase in Young's modulus, flexural strength, impact strength, hardness and thermal stability. Recently, Tawe et al. (2022) studied the mechanical behavior of composite material fabricated using keratin resin extracted from horn sheaths and reinforced with wood particles and horn sheaths particles, the sizes of which vary from 125 to 625 μm, respectively. It was observed that the best physical and mechanical properties were obtained at 225 μm. The wood particles/horn sheaths particles are stronger than horn sheaths particles/horn sheaths particles and can be used in a dry environment. Furthermore, the charactersitics of the bovine hoof were also recently investigated by Wang et al. (2021). Employing the nanoindentation and hierarchy structure of the bovine hoof wall, Wang et al. (2021) indicated that the bovine hoof wall has a layered structure, which effectively absorbs the energy released by the crack propagation and passivate the crack tip. It was also observed that the mechanical properties of the longitudinal direction specimens are stronger than those of the transverse direction specimens.

### Polyurethane as matrix

Polyurethane (PU) as a matrix of the biocomposites is one among the many important matrix materials employed. There are other matrix materials employed, such as: polypropylene (a thermoplastic), phenol formaldehyde and epoxy (both thermosetting plastics). Among these matrix materials (refer to Table 1), polypropylene shows reasonable tensile strength (32.63 MPa) and elongation at break (88.59%), demonstrating satisfactory flexibility. However, it exhibits lesser stiffness in comparison with that of the thermosetting plastics. In contrast, the phenol formaldehyde and epoxy display greater tensile strength (34.47 MPa and 42.56 MPa, respectively) and considerably greater tensile modulus (2757.9 MPa and 2076.52 MPa), indicating their rigid and brittle nature.

Also, it should be noted that the density and hardness values of these matrix materials vary substantially. Among these, polypropylene indicates the lowest density (0.911 g/cc), thus making it lightweight. Here, it should be noted that the thermosetting plastics such as phenol formaldehyde and epoxy display higher hardness (M93 and M80, respectively), with polypropylene material

**Table 1.** Properties of thermoplastic and thermosetting plastic polymer materials

| Properties | Polypropylene | Phenol formaldehyde | Epoxy | Pure PU |
|---|---|---|---|---|
| Ultimate tensile strength (MPa) | 32.63 | 34.47 | 42.56 | 8.31 |
| Tensile modulus (MPa) | 464.43 | 2757.9 | 2076.52 | 4.66 |
| Elongation at break (%) | 88.59 | 1.5 | 3.54 | 7.47 |
| Flexural strength (MPa) | 34.51 | 75.84 | 56.82 | - |
| Flexural modulus (MPa) | 459.34 | 3300 | 3640.34 | - |
| Izod impact strength (J/m) | 35.97 | 12.81 | 10.68 | 0.109 (J/mm$^2$) |
| Compression strength (MPa) | 37.92 | 82.74 | 189.86 | - |
| Hardness | R80 | M93 | M80 | 71.47 Shore hardness (D-scale) |
| Density (g/cc) | 0.911 | 1.2 | 1.132 | 1.081 |
| Water absorption (%) | 0.015 | 0.36 | 0.31 | 0.638 |

as softer (R80). However, the pure polyurethane possess very low tensile modulus (4.66 MPa) and elongation at break (7.47%). Accordingly, PU is less stiff but it was found to be more flexible.

On the polyurethane as matrix material of the composite, Chalivendra et al. (2003) studied the polyurethane cenosphere composites and observed that quasi-static stiffness in tension, compression and fracture toughness increased along with the cenosphere content. Pure polyurethane showed monotonic stiffening while that of 40% cenosphere by volume in polyurethane showed a stiffening-softening-stiffening behavior. The effect of size, content and interface of particle on the polymer composite properties was investigated by Fu et al. (2008). However, employing rice husk as reinforcement, Rozman et al. (2003) fabricated polyurethane composites with polypropylene glycol as polyol. They observed that the tensile and impact strength as well as swelling have increased up to a threshold weight percentage for smaller sized rice husk.

Xiong et al. (2006) while studying the mechanical and thermal behavior of multi-walled CNT reinforced polyurethane composite specimens observed that the properties were enhanced for 2% by weight of CNT and that CNT were dispersed with few clusters. Oprea (2011) investigated the varied weight percentage of agar filler reinforced castor oil based polyurethane composites and observed that the filler improves tensile strength and decreases breaking strains based on the filler content. Fornasieri et al. (2011) conducted experiments by chemically modifying wood-based polyurethane composite specimens and observed that tensile strength and Young's modulus increased, but the thermal stability did not. Hwang et al. (2016) compared the results of the mechanical properties obtained using finite element method and fabricated model of the carbon fiber fabric-reinforced polyurethane composites and observed that the results are in good agreement with Young's modulus. Similarly, the mechanical properties of carbon black/polyurethane composites was analyzed by Marhoon (2017a). From the investigation, it was observed that mechanical properties increased along with the carbon black content. Further, employing the sunflower husk particles, the experimental investigations was conducted to study the effect of sunflower husk particles reinforced polyurethane polymer matrix composites. It was observed that the optimum tensile strength, elasticity modulus and water absorption was obtained by adding 10% sunflower husk as a reinforcement material to polyurethane resin (Marhoon 2017b). Later, Najeeb (2020) reinforced the polyurethane using carbon nano tubes (CNT) and investigated the mechanical properties. From the anaylsis, it was observed that the composites with 1% weight percentage of CNT gives optimum results.

Keeping these properties of the bovine hoof and prospects of bovine hoof as reinforcement, this work aimed to evaluate the properties of bovine hoof reinforced composites. In other words, the objective of this work was to fabricate bovine hoof powder reinforced polyurethane composites, analyze their mechanical and tribological properties and determine the optimum loading of the hoof powder in the composites. Polyurethanes are used in fields such as automobile, structural, house appliances, etc. Polyurethanes are reaction polymers available in both thermoplastic and thermosetting polymers produced by reaction between di- or tri- poly-isocyanate with a polyol in the presence of catalyst or ultraviolet light. High amount of cross linking makes polymers hard and rigid while lesser amount of cross linking yields soft and elastic polymers.

## MATERIALS AND METHODS

### Materials and processing of bovine hoof powder

The bovine hooves were collected from local slaughterhouse at Vellore, Tamil Nadu, India. Polyol and isocyanate were procured from Veeyor Polymers Private Limited, Peenya, Bengaluru, India. The hooves collected from slaughterhouse were washed thoroughly in water, dipped in soap water, brushed to remove dirt and odor and dried in sunlight for two days. The hooves were cut into chips using a milling machine. The chips were pulverized using kitchen grinder. The bovine hoof powder was sieved using 250 μm and then using 125 μm sieves and the bovine hoof particle size ranging between 125 μm and 250 μm was used for the fabrication of composites. The bovine hoof powder was treated with 0.1 N NaCl for 8 hours, dried, defatted using diethyl ether for 4 hours, washed completely in water and dried. The defatted bovine hoof powder was treated with 0.1 N NaOH solution and dried. Figure 1 shows the photographs of hoof powder processing.

### Specimen preparation

Composites of varying weight percentages (0%, 2.5%, 5%, 7.5%, 10% and 15%) of bovine hoof powder-reinforced polyurethane were fabricated. The treated bovine hoof powder was mixed with polyether polyol using hot air and then with TDI hardener using mechanical stirrer. The powder mixed with resin was poured in to plate and disc shaped molds, applied with a releasing agent and allowed for a curing time of 90 minutes; afterwards, it was post cured at 110 °C in air oven for 16 hours. A plate-shaped composite specimen of 290 × 290 × 6 mm and disc shaped specimens of 55 mm diameter and thickness of 12 mm were fabricated. The plate-shaped composites were cut to the required size of the specimen as per ASTM standards. Figure 2 shows the manufacturing process of composites. Figure 3a to Figure 3c show the photographs of dies used for disc and plate shaped composites. Figure 3d shows the fabricated plate and disc shaped composites. Figure 4 shows the photographs of various test specimens.

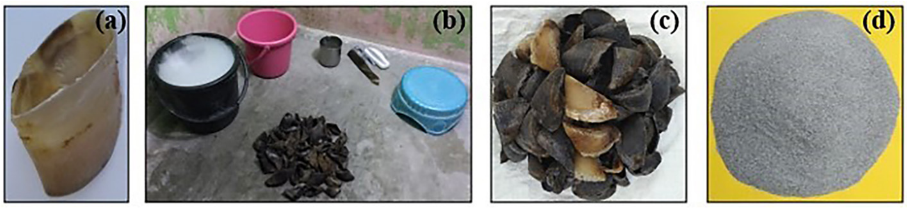


**Figure 1.** Photographs of hoof powder processing (a) raw hoof, (b) bovine hooves cleaned with soap water, (c) cleaned and dried hooves and (d) milled, ground and segregated bovine hoof powder

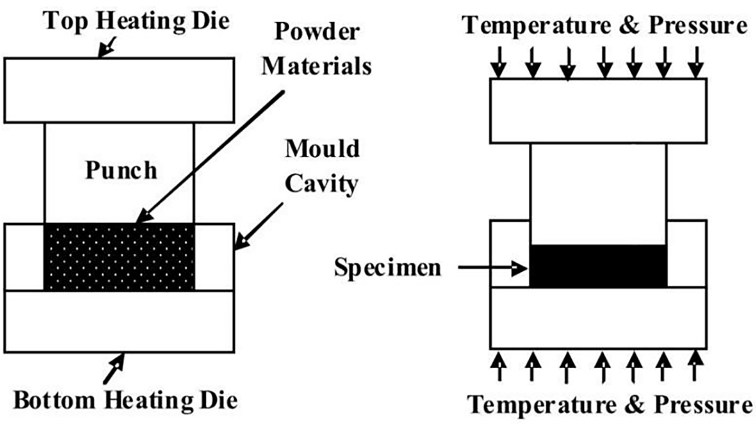


**Figure 2.** Manufacturing process of composites

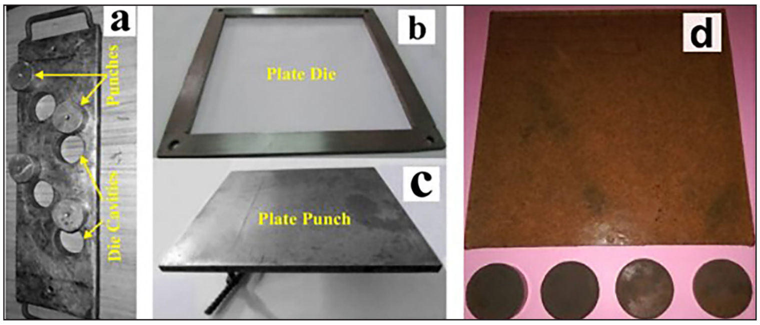


**Figure 3.** Photographs of (a) die and punch of disc shaped composites, (b) die of plate shaped composites, (c) punch of plate shaped composites and (d) fabricated plate and disc shaped composites

Figure 4a shows the tensile test specimen, Figure 4b shows the flexural test specimen, Figure 4c shows the impact test specimen, Figure 4d shows the specimens of hardness, pin-on-disc, density, water absorption, oil absorption and porosity tests, Figure 4e shows the specimens during tensile test and Figure 4f shows the specimens before and after the tensile test.

## Specimen testing

Mechanical and tribological properties such as tensile, flexural, impact, hardness, coefficient of friction, wear rate, density, porosity, water absorption and oil absorption properties were studied on specimens. Following the ASTM D638 standard, a tensile test was carried out on dog-bone shaped samples of 165 mm length, 3 mm thick and 12.7 mm width at the narrow section and 19 mm width at the widest section. A gauge length of 115 mm and cross head speed of 50 mm/min were used on universal testing machine. Following the ASTM D790 standard, 3-point bend type flexural testing was carried on specimens of 127 mm length, 12.7 mm width and 6 mm thick. A span length of sixteen times the thickness and a cross head speed of 2.6 mm/min were used on a universal testing machine. Following the ASTM D256

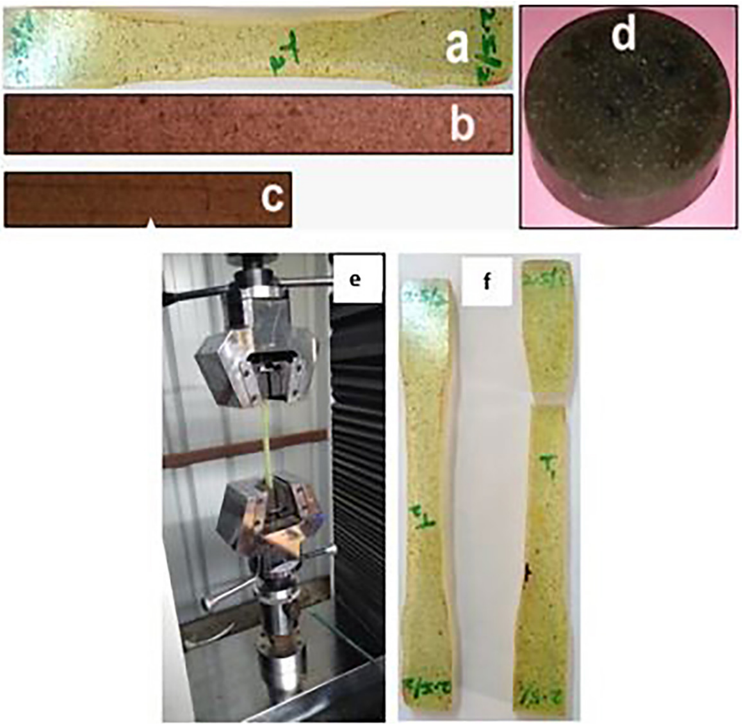


**Figure 4.** Photographs of composite specimens: (a) tensile test, (b) flexural test, (c) impact test, (d) hardness, pin-on-disc, density, water absorption, oil absorption and porosity tests, (e) during tensile test, (f) before and after tensile test

standard, an Izod impact test was carried on specimens of 63.5 mm length, 12.7 mm width and 6 mm thick. A V-notch angle of 45° for a depth of 2.54 mm was used on impact testing machine. Hardness test (Shore Hardness “D” Scale) was conducted on disc-shaped specimens of diameter 55 mm and 12 mm thick on Shore hardness testing machine.

Following the ASTM G99-05 standard, pin-on disc test was conducted to determine the coefficient of friction and wear rate on disc shaped specimens of diameter 55 mm, 12 mm thick and a through hole of 6 mm at the center. A stainless-steel pin of grade 304 with 6 mm diameter and 50 mm length was used. A 20 mm track radius, 1450 rpm spindle speed, 5 min time period and 911 m sliding distance was used on computerized pin-on-disc apparatus. Following the ASTM D792 standard, densities of the specimen were calculated according to the Archimedes principle using density measuring equipment. Following the ASTM D570-99 standard, water absorption percentage was calculated using the weights of dry specimens and specimens after 24 hours of immersion in water at room temperature. Following the ASTM D570-99 standard, oil absorption percentage was calculated using the weights of dry specimens and specimens after 24 hours of immersion in SAE 20/50 oil at room temperature. Porosity % was calculated using the weights of dry specimens and specimens after 8 hours of immersion in water at 100 °C. Specimens of diameter 55 mm and 12 mm thick were used for measuring the water absorption, oil absorption and porosity. SEM images were performed on Gold Palladium-coated tensile fractured surfaces with 10.0 kV accelerating voltage.

### Ultra violet (UV) weathering

The fabricated polyurethane composite specimen was exposed to accelerated UV weathering for 500 hours. To ensure uniform exposure of the UV radiation, the test sample of size 50 × 50 × 3 mm was attached at a distance of 10 cm from the UV source. Furthermore, it may be noted that no UV stabilizer was applied to investigate the degradation characteristics. The UV weathering was done in a controlled UV aging chamber constituting UVA-340 fluorescent lamps. Using these lamps, a solar radiation in the 295–400 nm range was simulated. The exposure to radiation was activated at 50 ± 2 °C with cycles consisting of 8 hours of UV irradiation at 0.89 W/m² (340 nm) which is followed by 4 hours of condensation at 40 ± 2 °C and 95% relative humidity. Accordingly, to characterize the modification that occurred due to the UV exposure, the Fourier Transform Infrared Spectroscopy (FTIR) analysis, in the range 4000–550 cm$^{-1}$, was carried out (as per ASTM D5477) and the results were discussed in the forthcoming sections.

## EXPERIMENTAL RESULTS

The results obtained from the testing for various mechanical and tribological properties of the BHP – PU composites are tabulated in Table 2. Also, the observations of these results were discussed in the following sections.

### Tensile strength

Tensile test graphs of varying weight % of BHP reinforced polyurethane composites is shown in Figure 5. Figure 5 (a) shows the chart of tensile strength of composites with varying wt% of BHP. From the chart, it was found that in increasing the BHP loading, the tensile strength increases up to 7.5 wt% and decreases thereafter. This is due to the fact that loading BHP particles up to 7.5% resists the movement of the matrix and thus increases the tensile strength. Increasing BHP loading beyond 7.5%, decreases the adhesion between

**Table 2.** Mechanical and tribological properties of composites

| Specimen composition (BHP: PU) | Tensile strength (MPa) | Tensile strain | Tensile modulus (MPa) | Impact strength (J/mm²) | Shore hardness (D-scale) | Coefficient of friction | Wear rate (g/m) × 10$^{-3}$ | Density (g/cc) | Porosity (%) | Water absorption (%) | Oil absorption (%) |
|---|---|---|---|---|---|---|---|---|---|---|---|
| 0:100 | 8.31 | 7.47 | 4.66 | 0.109 | 71.47 | 1.03 | 0.28 | 1.081 | 0.97 | 0.638 | 0.601 |
| 2.5:97.5 | 2.36 | 9.53 | 0.58 | 0.064 | 68.79 | 1.26 | 0.55 | 1.091 | 1.035 | 0.698 | 0.758 |
| 5:95 | 2.43 | 10.15 | 0.67 | 0.063 | 66.79 | 1.276 | 0.87 | 1.099 | 1.102 | 0.718 | 0.777 |
| 7.5:92.5 | 3.05 | 11.64 | 0.73 | 0.06 | 65.29 | 1.49 | 1.04 | 1.109 | 1.095 | 0.772 | 0.816 |
| 10:90 | 1.33 | 5.54 | 0.90 | 0.059 | 64.17 | 0.9 | 1.16 | 1.116 | 1.198 | 0.816 | 0.826 |
| 15:85 | 0.81 | 1.28 | 1.04 | 0.057 | 62.27 | 0.5 | 1.21 | 1.135 | 1.219 | 0.839 | 0.844 |

the particles and the matrix due to insufficient matrix material and thus decreases the tensile strength. Figure 5b shows the stress strain graphs of tensile test of varying wt% of BHP reinforced polyurethane composites. From the graphs it is observed that the tensile strength of the composites increases up to 7.5% and decreases thereafter. Figure 5c shows chart of strain values of composites with varying wt% of BHP. From the chart, it is observed that the tensile strain increases up to 7.5% and decreases thereafter. Figure 5d shows the chart of tensile modulus of composites with varying weight % of BHP. From the chart, it is observed that tensile modulus increases continuously with increase in BHP loading. This is due to the fact that modulus depends on particle loading and not on the particle-matrix adhesion, as observed by Fu et al. (2008).

### Impact strength

Figure 6 shows the chart of impact strength of composites with varying wt% of BHP. From the chart, it is observed that the impact strength of the composite specimens decreases when increasing the BHP loading. This is due to the fact that loading of BHP particles acts as stress raisers and assists the formation of cracks and thus decreases impact strength.

### Hardness and wear rate

The evaluation of Shore hardness (D Scale) of composites with varying wt% of BHP (as shown in Figure 7a) indicates that increasing BHP loading results in a decrease in the hardness of composites. This is due to the fact that BHP particles are less hard than the polyurethane and thus increase in BHP loading decreases hardness. Figure 7b shows the chart of wear rate of composites with varying wt% of BHP. From the chart, it is observed that wear rate increases with increase in BHP loading. This behavior may be attributed to the hardness of BHP, which is lesser than that of polyurethane.

### Coefficient of friction

The coefficient of friction of composites with varying wt% of BHP is shown in Figure 8. From

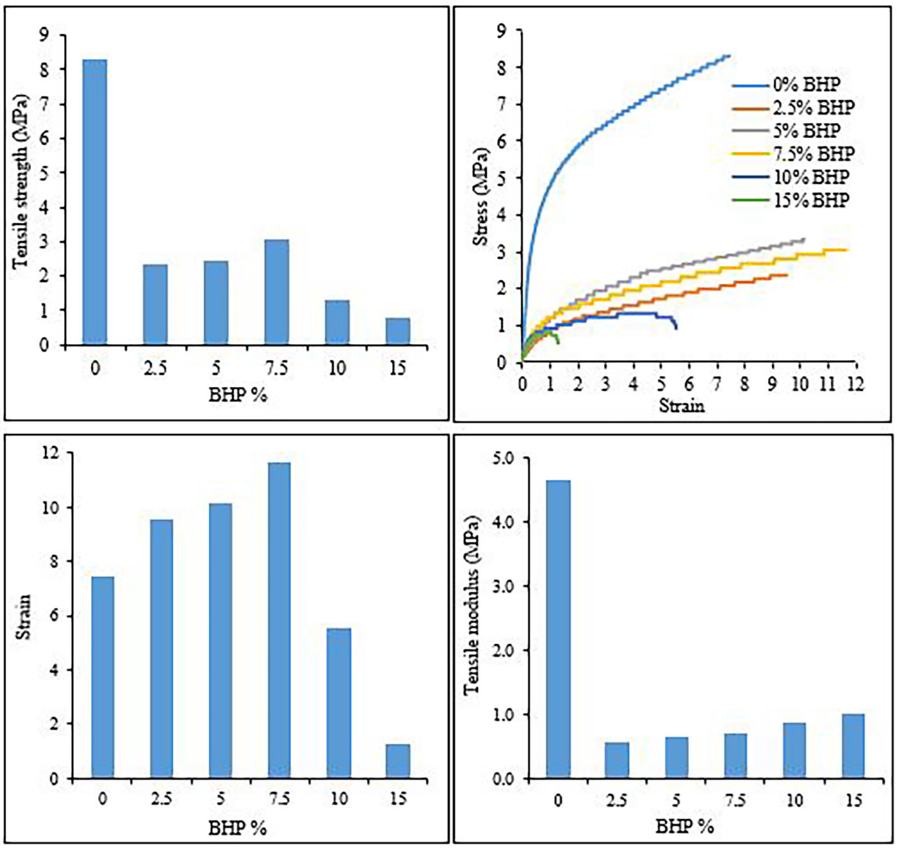


**Figure 5.** Tensile test graphs of varying wt% of BHP reinforced polyurethane composites (a) tensile strength, (b) stress-strain graph, (c) strain and (d) tensile modulus

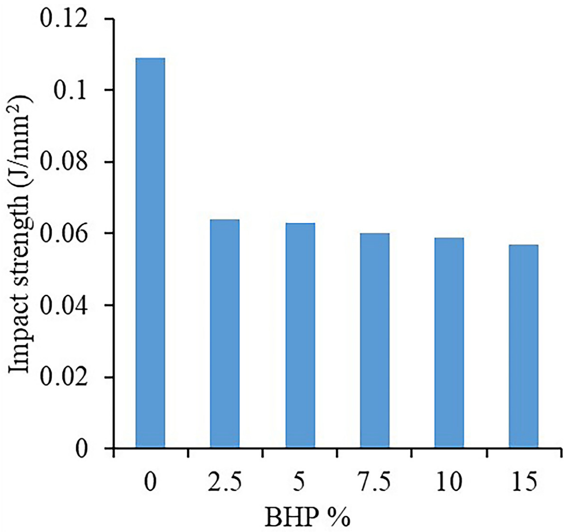


**Figure 6.** Impact strength of varying wt% of BHP reinforced polyurethane composites

the chart, it is observed that the coefficient of friction of the composites increases along with BHP loading up to 7.5% by weight and decrease thereafter. This is due to the fact that the bonding strength between BHP and polyurethane is good up to 7.5% by weight and decreases thereafter due to lack of polyurethane matrix.

## Density and porosity

Figure 9a shows the chart of density with varying weight % of BHP. From the chart, it may be observed that the density of the composites increases along with the BHP percenatge. This could be due the fact that the density of the BHP is higher than polyurethane. Figure 9b shows the chart of porosity % of composites with varying weight % of BHP. From the chart, it is found that, porosity % of the composites increases along with the BHP loading. This is due to the fact that micro cavities are formed with increase in BHP loading, leading to the increase in pores and hence increases porosity percentage.

## Water and oil absorption

The water absorption % of composites with varying wt% of BHP is shown in Figure 10a. From the chart, it was found that the water absorption % of the composites increases along with increasing BHP loading. This is due to the fact that micro cavities are formed with increase in BHP loading, leading to the increase in pores and hence increase water absorption percentage. A chart showing oil absorption percentage of composites with varying wt% of BHP is shown in Figure 10b. From the chart, it was found that oil absorption % of the composites increases in increasing the BHP loading. This is due to the fact that, micro cavities

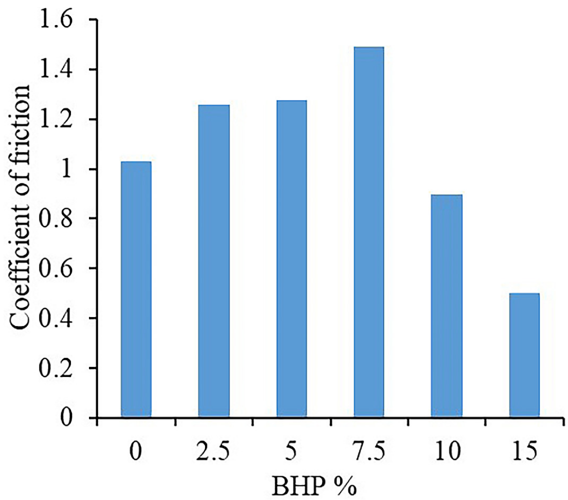


**Figure 8.** Coefficient of friction vs wt% of BHP reinforced polyurethane composites

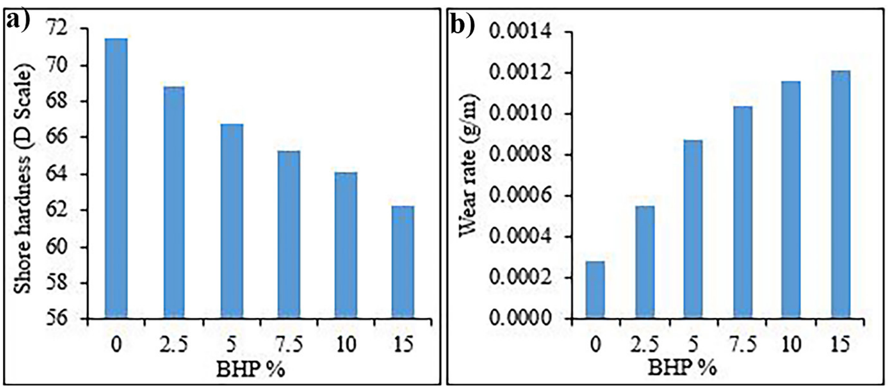


**Figure 7.** Shore hardness; wear rate of BHP reinforced polyurethane composites

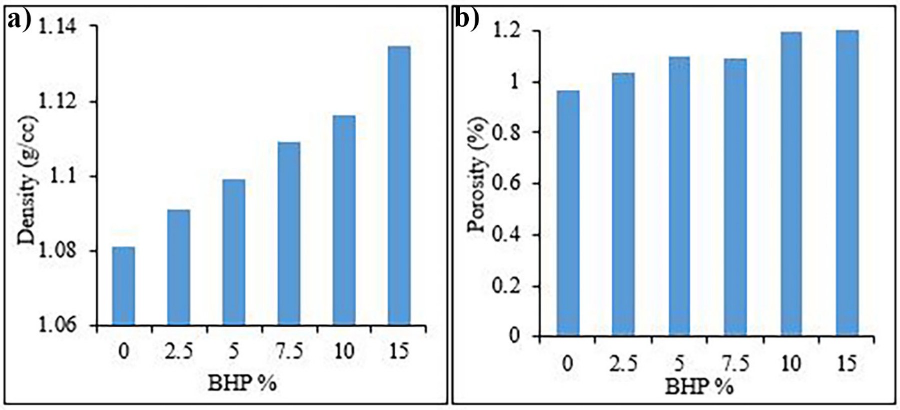


**Figure 9.** Density and porosity of BHP reinforced polyurethane composites

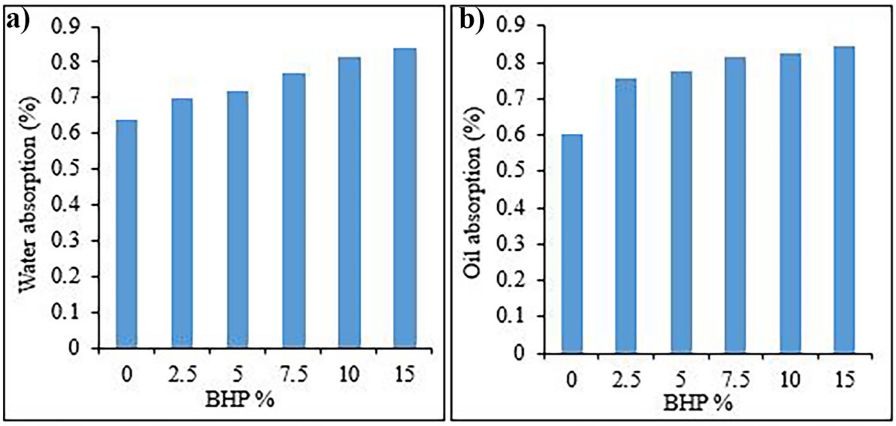


**Figure 10.** Water and oil absorption of varying wt% of BHP reinforced polyurethane composites

are formed with increase in BHP loading, leading to the increase in pores and hence increases oil absorption percentage.

### Degradation analysis using fourier transform infrared spectroscopy (FTIR)

To evaluate the degradation using FTIR, the BHP was tested initially (Figure 11). From the figure, it may be noted that BHP displays distinctive peaks conforming to the functional groups available in keratin-based fibers. In general, in keratin based biomaterials, the absorption bands at 533.35 cm$^{-1}$, 466.77 cm$^{-1}$, and 412.77 cm$^{-1}$ are related to skeletal deformations and bonding vibrations. The broad absorption band observed at 3271.27 cm$^{-1}$ may possibly relate to the broadening vibrations of O–H and N–H groups. This shall be considered as an indication of the existence of hydroxyl and amide groups. Here, it should be noted that the peak observed at 2927.94 cm$^{-1}$ may be attributed to C–H stretching vibrations of aliphatic hydrocarbons. Also, a noticeable peak at 1631.78 cm$^{-1}$ resembles C=O stretching in amides (amide I band). Such characteristics confirms the existence of peptide linkages. Furthermore, the absorption band at 1516.05 cm$^{-1}$ signifies the N–H bonding and C–N stretching (amide II band). This behavior is characteristic of proteinaceous materials. Similarly, the peaks at 1384.89 cm$^{-1}$ and 1234.44 cm$^{-1}$ indicates C–N stretching and N–H bonding vibrations of amide III, generally related with structures of keratin proteins. The peak at 1053.13 cm$^{-1}$ corresponds to C–O–C stretching due to either carbohydrate components or other negligible components in BHP fibers.

Figure 12 shows the spectral shifts representing hydrogen bonding of urethane and keratin that clearly signifies the successful incorporation of bovine hoof fibers into the polyurethane matrix. Such interactions between the matrix and reinforcement improves adhesion, dispersion, and interfacial bonding. Therefore, resulting in the composite with chemical

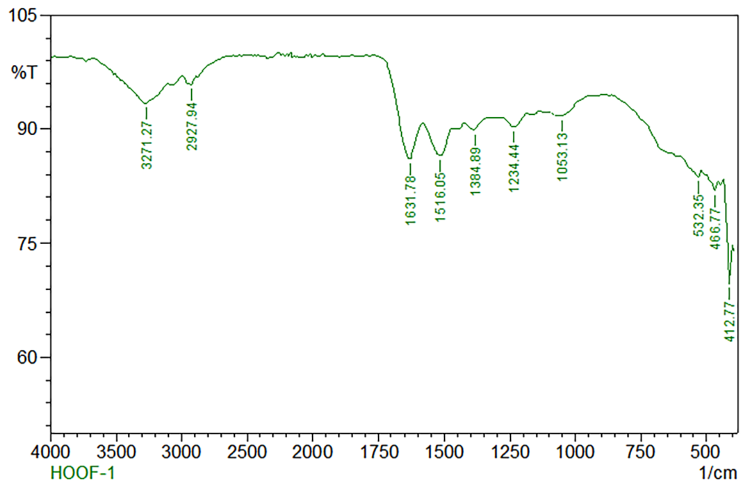


**Figure 11.** FTIR spectra of Bovine hoof powder

integrity, mechanical and tribological properties. However, either the structural rearrangements or keratin degradation may possibly modify the absorption bands.

Furthermore, the FTIR spectra indicate (Figure 12) that UV weathering induce shifts in carbonyl (1724 cm⁻¹) and amide (1527 cm⁻¹) peaks. Also, the persistence of the amide II band suggests partial keratin stability. Similar behavior was observed by Andrady et al. (2023) while investigating polyurethane/keratin composites. That is, the UV exposure normally damages urethane bonds and interrupts hydrogen networks. Nevertheless, the reduction of C-O-C peak of 1099 cm⁻¹ is found to be in contrast with the generally reporting stable ether linkages. This indicate matrix-specific degradation pathways. Though, the keratin is found to be resilient compared to PU, as a whole, the analysis demonstrate the weakening of interfacial bonding due to UV weathering. It should be noted that no UV stabilizer was employed, consequently, the polyurethane composite may experience faster photodegradation. Accordingly, the UV radiation may possibly result in oxidative degradation, chain scission, and hydrolysis. Further detailed investigation is required to characterize the degradation.

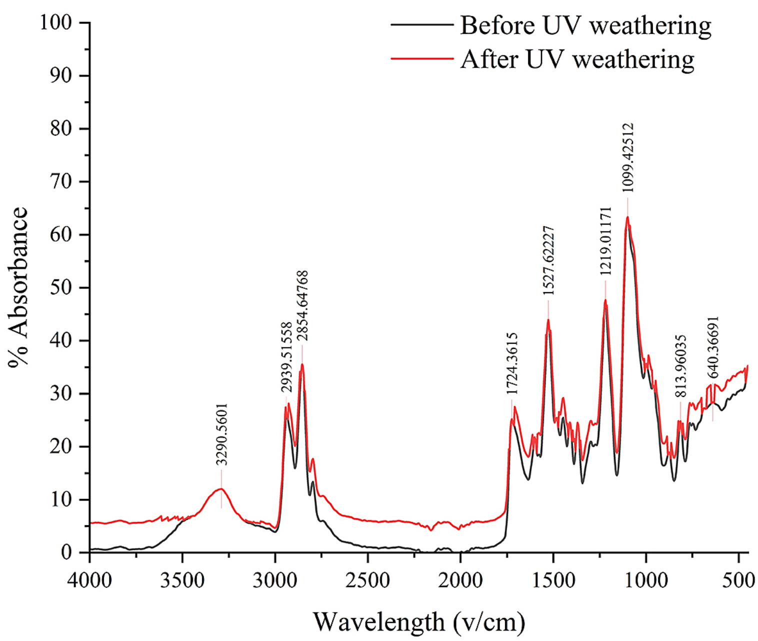


**Figure 12.** FTIR spectra of BHP – PU composites

### Scanning electron microscopy

SEM micrographs of tensile fractured surfaces of varying weight percentage of BHP reinforced polyurethane composites are shown in Figure 13. The micrographs were taken at a magnification of 200x, at a scale of 200 µm and at an accelerating voltage of 10.0 kV. From the micrographs, it is observed that at low weight percentages of BHP, the distribution of particles in polyurethane matrix is even and with increase in weight percentage, agglomeration of the particles increases and failure of the composites takes place due to insufficient amount of polyurethane matrix to cover the particles. Also, due to the formation of cracks that arises from micro-cavities and de-bonding, failure of the composites takes place. By the nucleation of micro-cracks at the interfacial sites, crack propagation takes place and it increases with BHP content due to weak interface between BHP and matrix.

## RESULTS ANALYSIS

From the investigation of the mechanical and tribological properties of polyurethane composites reinforced with varying weight percentages

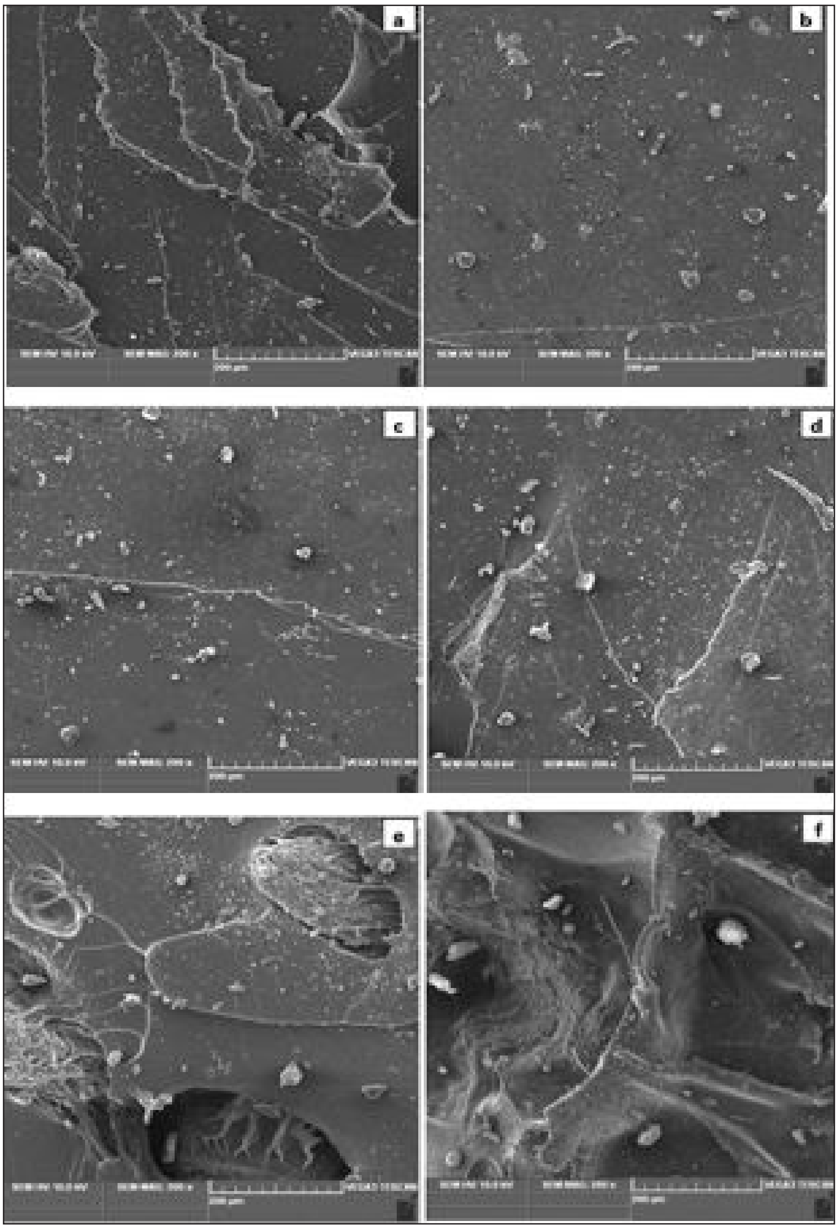


**Figure 13.** SEM micrographs of tensile fractured surfaces of varying wt% of BHP reinforced polyurethane composites: (a) 0% BHP, (b) 2.5% BHP, (c) 5% BHP, (d) 7.5% BHP, (e) 10% BHP and (f) 15% BHP

of bovine hoof powder, it was found that with the increase of BHP percentage, the tensile strength of the composites increases up to 7.5%. This improvement may be attributed to the presence of BHP particles,which possibly restrict the movement of the matrix, thereby increasing strength. Nevertheless, in case of BHP percentage exceeding 7.5%, the tensile strength decreases due to inadequate matrix material. Also, this may weaken the process of adhesion between the reinforcement particles and the matrix material. Likewise, the tensile strain follows the similar trend, with a maximum of 7.5% and declining afterwards. In contrast, the tensile modulus continuously increases with higher BHP weight percentage, since it depends on the amount of the reinforcement particle rather than the bonding between the reinforcement and the matrix.

The impact strength of the composites, however, decreases with increasing BHP loading. This is because the BHP particles act as stress concentrators, stimulating crack development and decreasing the material's ability to endure impact. Moreover, the hardness of the composites decreases as the BHP content increases. Meanwhile BHP particles are softer than the polyurethane matrix, their integration reduces the hardness of the material. The coefficient of friction originally increases with BHP loading up to 7.5%, due to durable bonding between the particles and the matrix. Away from this point, the coefficient of friction decreases due to inadequate matrix material, which deteriorates the bonding strength.

The wear rate of the composites rises with higher BHP percentage, since the bovine hoof powder is not very hard compared to that of the polyurethane matrix. Therefore, the composites are expected to experience higher wear. Instead, the density of the composites increases with the increase in BHP content. This is due to the fact that BHP is of a higher density than polyurethane matrix. Also, the porosity increases with higher BHP percentage. This may be attributed to the presence of possible micro-cavities and pores in the composite. Such increase in the porosity additionally contributes to greater water and oil absorption characteristics. It should be noted that the existence of micro-cavities or pores possibly provides passages for liquids to infiltrate the composite.

Furthermore, from the above investigations, and the comparative analysis of various matrices and reinforcements, it may be inferred that the modification in properties of composites depends on the interaction of the matrix and the reinforcements. For example, polypropylene indicates stiffening fillers that enhance both tensile and flexural modulus, however there is decrease in ductility. reinforcements. In phenol formaldehyde, there is a reduction in tensile strength. However, the elongation characteristics indicate the reinforcmeets induced "plasticization". In comparison, the epoxy-based hybrids demonstrate better compatibility between matrix and reinforcement. In comparison with these three matrices, the PU shows reduction in rigidity with increased elasticity. It should be noted that in all cases of matrices, there is a reduction in the impact strength.

Comparing various biocomposites (refer to Tables 3 and 4), it may be noted that the BHP/PU composites indicate reasonable hardness, excellent coefficient of friction and low wear resistance. Since, the BHP/PU composites are also lightweight and less porous, accordingly, such composites may be employed in applications with no abrasions. Here, it should be noted that HP/Epoxy indicates high hardness and compression strength, thus may be considered for high-load applications. However, the HP/PF composites indicate good wear resistance and low friction. Also,

**Table 3.** Mechanical properties of the horn powder composites and bovine hoof composites

| Properties | Polypropylene (PP) | Horn powder (HP) & PP | Phenol formaldehyde (PF) | Horn powder & PF | Epoxy | Horn powder & epoxy | Polyurethane (PU) | Bovine hoof powder & PU |
|---|---|---|---|---|---|---|---|---|
| TS (MPa) | 32.63 | 27.68 | 34.47 | 12.58 | 42.56 | 28.4 | 8.31 | 3.05 |
| TM (MPa) | 464.43 | 537.52 | 2757.9 | 1252 | 2076.52 | 998.76 | 4.66 | 0.73 |
| EAB (%) | 88.59 | 13.58 | 1.5 | 3.48 | 3.54 | 3.17 | 7.47 | 11.64 |
| FS (MPa) | 34.51 | 40.28 | 75.84 | 56.73 | 56.82 | 52.38 | - | - |
| FM (MPa) | 459.34 | 625.29 | 3300 | 5739 | 3640.34 | 3722.55 | - | - |
| IS (J/m) | 35.97 | 15.99 | 12.81 | 8.56 | 10.68 | 7.54 | 0.109 J/mm$^2$ | 0.06 J/mm$^2$ |
| Density (g/cc) | 0.911 | 0.955 | 1.2 | 1.95 | 1.132 | 1.146 | 1.081 | 1.109 |

**Table 4.** Tribological properties of the horn powder composites and bovine hoof composites

| Tribological properties of composites | | | |
|---|---|---|---|
| Properties | HP/PF<br>425 µm & 15% | HP/Epoxy<br>425 µm & 15% | BHP/PU<br>125–250 µm & 7.5% |
| Hardness | 33.86 (HRB) | 82.83 (HRL) | 65.29 Shore Hardness (D-Scale) |
| Compression strength (MPa) | 125.94 | 165.08 | - |
| Coefficient of friction | 0.346 | 0.72 | 1.49 |
| Wear rate (g/m) | 2.22E-5 | 5.96E-5 | $1.04 \times 10^{-3}$ |
| Surface roughness (µm) | 1.578 | 1.662 | - |
| Density (g/cc) | 1.95 | 1.146 | 1.109 |
| Porosity (%) | 2.72 | 1.677 | 1.095 |
| Water absorption (%) | 0.38 | 0.632 | 0.772 |
| Oil absorption (%) | 0.64 | 0.829 | 0.816 |

note that the HP/PF reveals the better durability with less fluid absorption, high density, and good wear characteristic – ideal for tough working conditions. Microstructural examination reveals that at lesser BHP content, the particles are uniformly distributed within the matrix. Nevertheless, as the BHP content rises, particle accumulation occurs, and the matrix is inadequate to entirely shield the particles. This effects in the formation of micro-cavities and de-bonding. This phenomenon induces the initiation of cracks. Therefore, the crack transmission is more distinct at higher BHP percentages due to the fragile interface between the reinforcement particles and the matrix, eventually resulting in the failure of material.

The present investigation demonstrated that 7.5% BHP loading signifies a critical threshold for optimizing the properties of polyurethane composites. Though BHP reinforcement improves certain properties, such as tensile strength and modulus, disproportionate loading leads to degradation in impact strength, hardness, wear resistance, and absorption characteristics. The results also highlight the significance of matching BHP content to attain the anticipated performance of polyurethane composites.

## CONCLUSIONS

A novel composite is fabricated successfully using biowaste and tested for mechanical and tribological properties. From the analysis, the following observations and inferences may be made.

- The tensile strength, tensile modulus, coefficient of friction, density, porosity, water absorption and oil absorption increase with increase in BHP loading.
- Wear rate, hardness and impact strength decrease with increase in BHP loading.
- Increase in coefficient of friction and decrease in wear rate are beneficial for tribological application.
- The SEM images indicate uniform dispersion of particles in polyurethane matrix at low BHP weight percentage.
- A stiffening-softening-stiffening behavior of composites is observed with increase in loading of BHP from pure polyurethane.
- Mechanical properties are found to be optimum for 7.5% BHP in polyurethane composites.
- The water absorption tests demonstrated increased hydrophilicity. Thus, possibily resulting in the faster deterioration of the composites.
- The UV weathering and subsequent FTIR investigation characterized the degradation and indicated oxidation process at 1724 $cm^{-1}$ and 1600 $cm^{-1}$.
- There is enhancement of surface roughness and development of microcracks due to UV weathering. This could be attributed to to photolytic and hydrolytic effects.
- More studies may be conducted employing the UV stabilizers, to characterize the degradation.

Given the above discussed mechanical and tribological properties of fabricated bovine hoof powder-reinforced composites, the resulting composites may find suitable utility in applications like footwear etc. Thus, such use of animal based biowaste shall not only ecological friendly and cost effective, but also facilitates attaining UN- Sustainable Development Goals.

## Acknowledgements

We acknowledge the support of the Management of C. Abdul Hakeem College of Engineering and Technology, Melvisharam-632 509, India. towards conducting this research work. Also, we are indebted to the support of Center for Sustainable Energy and Waste Management, faculty members and staff of the Department of Mechancal Engineering towards the conduct of experiments for this work.


## REFERENCES


1. Andrady, A.L., Heikkilä, A.M., Pandey, K.K. *et al.* Effects of UV radiation on natural and synthetic materials. *Photochem Photobiol Sci* 22, 1177–1202 (2023). https://doi.org/10.1007/s43 630-023-00377-6
2. Baillie, C., Southam, C., Buxton, A., Pavan, P. (2000). Structure and properties of bovine hoof horn. *Advanced Composites Letters*, *9*(2), 101–113.
3. Chalivendra, V.B., Shukla, A., Bose, A., Parameswaran, V. (2003). Processing and mechanical characterization of lightweight polyurethane composites. *Journal of Materials Science, 38*, 1631–1643.
4. Fornasieri, M., Alves, J.W., Muniz, E.C., Ruvolo-Filho, A., Otaguro, H., Rubira, A.F., Carvalho, G.M. (2011). Synthesis and characterization of polyurethane composites of wood waste and polyols from chemically recycled pet. *Composites: Part A, 42*, 189–195.
5. Fu, S., Feng, X., Lauke,B., Mai, Y. (2008). Effects of particle size, particle/matrix interface adhesion and particle loading on mechanical properties of particulate-polymer composites. *Composites: Part B, 39*, 933–961.
6. Huang, W., Yaraghi, N.A., Yang,W., Velazquez-Olivera,A., Li, Z., Ritchie,R.O., Kisailus,D., Stover, S., McKittrick, J. (2019). A natural energy absorbent polymer composite: The equine hoof wall. *Acta Biomaterialia*, *90*, 267–277.
7. Hwang, S., Liu, H. (2016). Prediction of elastic constants of carbon fabric/polyurethane composites. *Solid State Phenomena, 258*, 233–236.
8. Issa, K., Idris, M.H., Tikau, M.I. (2020). Animal wastes as thermoplastic composite reinforcement materials for sustainable development. *International Journal of Innovative Technology and Exploring Engineering, 9*(10), 62–66.
9. Kumar, D., Rajendra Boopathy, S., Sangeetha, D., Bharathiraja, G. (2017). Investigation of mechanical properties of horn powder-filled epoxy composites. *Strojniški vestnik-Journal of Mechanical Engineering, 63*(2), 138–147.
10. Kumar, D., Muruganandhan, R., Thirumavalavan, K. (2020). Optimization of mechanical and thermal properties of biowaste horn powder reinforced phenol formaldehyde composites. *Interciencia Journal, 45*(1), 263–268.
11. Kumar, D., Rajendra Boopathy, S. (2014). Mechanical and thermal properties of horn fibre reinforced polypropylene composites. *Procedia Engineering, 97*, 648–659.
12. Kumar, D., Rajendra Boopathy, S., Sangeetha, D. (2016). Investigation on Tribological Properties of Horn Fibre Reinforced Epoxy Composites. *International Journal of Mechanical & Mechatronics Engineering, 16*(3), 79–88.
13. Marhoon, I.I. (2017a). Mechanical and physical properties of polyurethane composites reinforced with carbon black N990 particles. *International Journal of Scientific & Technology Research, 6*(8), 225–228.
14. Marhoon, I.I. (2017b). Effect of sunflower husk particles added to polyurethane polymer matrix composite. *International Journal of Scientific & Technology Research, 6*(8), 174–176.
15. Najeeb, H.S.A. (2020). Influence of carbon nanotubes on mechanical properties of polyurethane composites. *Journal of Pollution Effects & Control, 8*(5), 1–5.
16. Olokode, O.S., Fakolujo, S.O., Aiyedun, P.O., Jaji, Z.O., Owoeye, F.T., Anyanwu, B.U. (2012). Experimental study on the morphology of keratin based material for asbestos free brake pad. *Journal of Basic & Applied Sciences, 8*, 302–308.
17. Olszewski, A., Nowak, P., Kosmela, P., Piszczyk, L. (2021). Characterization of highly filled glass fiber/carbon fiber polyurethane composites with the addition of bio-polyol obtained through biomass liquefaction. *Materials, 14*(6), 1–15.
18. Oprea, S. (2011). Preparation and characterization of the agar/polyurethane composites. *Journal of Composite Materials, 45*(20), 2039–2045.
19. Rozman, H.D., Ang, L.G., Tay, G.S., Abubakar, A. (2003). The mechanical properties of rice husk-polyurethane composites. *Polymer-Plastics Technology and Engineering, 42*(3), 327–343.
20. Tawe, L., Gaga, D. B., Zakary, Y., Karga, T. L., Danwe, R. (2022). Mechanical behaviours of composite material manufactured with beef horn sheath's adhesives. *American Journal of Engineering Research, 11*(1), 48–53.
21. Wang, B., Huang, Y., Zhou, B., Li, W., Chen, H. (2021). Nanoindentation and Hierarchy Structure of the Bovine Hoof Wall. *Materials, 289*(14), 1–13.
22. Xiong, J., Zheng, Z., Qin, X., Li, M., Li, H., Wang, X. (2006). The thermal and mechanical properties of a polyurethane/multi-walled carbon nanotube composite. *Carbon, 44*, 2701–2707.
23. Yilma, K.T., Tesfaye, T., Enawgaw, H., Ayele, M., Limeneh, D.Y., Gibril, M., Kong, F. (2022). Optimizing the extraction of keratin from cattle hoof using central composite design. *Advances in Materials Science and Engineering,* 1–12.